

8-2015

# INERTIAL PARTICLE DYNAMICS IN SIMPLE VORTEX FLOW CONFIGURATIONS

Senbagaraman Sudarsanam

*Clemson University*, [ssudars@g.clemson.edu](mailto:ssudars@g.clemson.edu)

Follow this and additional works at: [https://tigerprints.clemson.edu/all\\_theses](https://tigerprints.clemson.edu/all_theses)



Part of the [Engineering Commons](#)

---

## Recommended Citation

Sudarsanam, Senbagaraman, "INERTIAL PARTICLE DYNAMICS IN SIMPLE VORTEX FLOW CONFIGURATIONS" (2015).

*All Theses*. 2186.

[https://tigerprints.clemson.edu/all\\_theses/2186](https://tigerprints.clemson.edu/all_theses/2186)

This Thesis is brought to you for free and open access by the Theses at TigerPrints. It has been accepted for inclusion in All Theses by an authorized administrator of TigerPrints. For more information, please contact [kokeefe@clemson.edu](mailto:kokeefe@clemson.edu).

# INERTIAL PARTICLE DYNAMICS IN SIMPLE VORTEX FLOW CONFIGURATIONS

---

A Dissertation  
Presented to  
the Graduate School of  
Clemson University

---

In Partial Fulfillment  
of the Requirements for the Degree  
Master of Science  
Mechanical Engineering

---

by  
Senbagaraman Sudarsanam  
August 2015

---

Accepted by:  
Dr. Phanindra Tallapragada, Committee Chair  
Dr. Ethan Kung  
Dr. Michael M. Porter

# Abstract

Inertial Particle Dynamics In Simple Vortex Flow Configurations

Senbagaraman Sudarsanam

Dynamics of inertial particles differ significantly from that of the underlying fluid flow. This difference in the dynamics of Inertial particles from that of fluid tracers can be exploited to segregate particles by size. While external forces can be used to manipulate the dynamics of such particles, using hydrodynamic forces which are always present in the flows of interest to manipulate inertial particle dynamics offers several advantages. Vorticity is one such phenomenon that is frequently encountered in natural and industrial flows. Thus, the dynamics of inertial particles have been studied in the presence of simple vortex flow configurations in this work, with the aim of gaining better insight into the problem of achieving size based segregation in the presence of vortex flow fields.

In the first problem that has been investigated, the dynamics of inertial particles with varying stokes numbers have been studied in a four vortex flow configuration. After stating criteria to ensure that the particles have non-trivial dynamics, the criteria has been used to separate heavy particles from light particles using an array of vortices.

The second problem studied is that of particle focusing in microfluidic chan-

nels. It is well known that inertial particles in the presence of hydrodynamic forces in microfluidic channel flows, focus into thin bands which can be used to achieve size based separation of such particles. One such force is the force exerted by dean vortices that form in flows through curved micro channels. In this study, we seek to computationally demonstrate that at low Reynolds numbers, particles with higher stokes number tend to cluster around the dean vortices, and thus leading to focused bands in the flow, while lighter particles are dispersed in the channel.

While there exists two well established criteria to identify regions in phase space which permit inertial particles to lose their relative velocities and settle down, we introduce a third criteria to identify regions of the four dimensional phase space comprising of two dimensional space and the components of relative velocity in each of the two dimensions, within which the relative velocity of inertial particles may decay with time.

# Dedication

I dedicate this work to my parents, Sudarsanam and Sumathi for their love and support.

# Acknowledgments

I owe my deepest gratitude to my advisor Dr.Phanindra Tallapragada for his guidance, support and encouragement. I would like to thank him for being my friend, critic and mentor and for the endless patience he has shown in helping me learn and grow. My experience working with him has been an eye opener and the time spent working with him will always be cherished. I would like to take this opportunity to thank him for the part he has played in making me a better student, a competent researcher and a keen thinker. I would also like to thank Dr.Ethan Kung and Dr.Michael Porter for being on my committee.

I owe my gratitude to Faculty members Mr.Balaji.K and Dr.Pradeep Kumar(Now at the Indian Institute of Space Science and Technology) at Amrita Vishwa Vidyapeetham University who instilled the spirit of scientific inquiry in me.

Among my peers at Clemson, I would like to thank my friends Ashwin Srinath and Neelakantan Padmanabhan to whom I owe my interest in scientific computing, for their patience with my innumerable questions and also for wonderful discussions about engineering in general. I thank my research group mates Nilesh Hasabnis and Ketaki Joshi for being interesting and knowledgeable people to work with. I would also like to thank my roommates Kaushik Mohan and Vishal Elangovan who have always been there to offer words of encouragement during testing times.

Most Importantly, I would like to thank my parents, my family and God to

whom I owe everything.

# Table of Contents

<b>Title Page</b> . . . . .	<b>i</b>
<b>Abstract</b> . . . . .	<b>ii</b>
<b>Dedication</b> . . . . .	<b>iv</b>
<b>Acknowledgments</b> . . . . .	<b>v</b>
<b>List of Figures</b> . . . . .	<b>ix</b>
<b>1 Introduction</b> . . . . .	<b>1</b>
1.1 Background . . . . .	1
1.2 Motivation . . . . .	2
1.3 Thesis Contributions . . . . .	6
1.4 Thesis Organization . . . . .	7
<b>2 Review of Theory</b> . . . . .	<b>9</b>
2.1 Review Of Point Vortex Dynamics . . . . .	9
2.2 Other Approximate Models Of Vorticity . . . . .	13
2.3 Milne Thomson Circle Theorem . . . . .	17
2.4 Review Of Inertial Particle Flows . . . . .	18
<b>3 Computational Methodology</b> . . . . .	<b>23</b>
3.1 Runge-Kutta Fourth Order Scheme . . . . .	23
3.2 Four Vortex Configuration . . . . .	23
3.3 Particles In a Confined Geometry . . . . .	24
<b>4 Results and Discussion</b> . . . . .	<b>27</b>
4.1 Sensitivity Field Of Relative Velocity . . . . .	28
4.2 Size Based Segregation of Particles Using an Array of Oscillating Cylinders . . . . .	33
4.3 Inertial Particle Focusing In A Circular Cylinder . . . . .	37
4.4 A New Criteria For Inertial Particles To Settle Down Onto Streamlines . . . . .	39



5 Conclusions and Future Work . . . . .	44
Bibliography . . . . .	46

# List of Figures

1.1	Vibrating cylinder in stationary fluid, $x(t) = A\sin(\omega t)$ . . . . .	4
1.2	The top row shows particles of $45\mu$ m at various Reynolds numbers and the lower row shows the $95\mu$ m particles at the corresponding Reynold number, flowing through a curved channel . . . . .	6
2.1	Velocity field generated by a single vortex at the origin . . . . .	13
2.2	Velocity field generated by a four vortex configuration . . . . .	14
2.3	Velocity profile of a rankine vortex . . . . .	15
2.4	Velocity profile of a Lamb-Oseen vortex . . . . .	17
2.5	Streamlines of a 2-vortex flow . . . . .	18
2.6	Stream lines of a 2-vortex flow with cylinder . . . . .	18
3.1	The four vortex configuration used to investigate particle trapping using vibrating cylinders . . . . .	24
3.2	Vector $w$ is the reflected vector and $v$ is the incident vector related by $w = v - 2(v \cdot \hat{n})\hat{n}$ . . . . .	25
3.3	Trajectory of a particle reflecting off boundary walls . . . . .	26
4.1	Binary plots of regions with $Re(\lambda) - \frac{2}{3St} > 0$ in gray and $Re(\lambda) - \frac{2}{3St} < 0$ in white for various stokes numbers . . . . .	29
4.2	Particles of different stokes numbers settling down into periodic orbits of different radii around a vortex . . . . .	32
4.3	Particles of different sizes trapped at the vortex cores in a four vortex flow . . . . .	35
4.4	Distribution of particles of a range of stokes numbers in a vortex array . . . . .	36
4.5	Relative velocity sensitivity field for particles over a range of stokes numbers (Left) and the corresponding distribution of a set of particles after time 't'(Right) . . . . .	38
4.6	A contour of the angle $\theta$ by which the unstable eigen vector of $-(j + \mu I)$ rotates about the x-axis with special case and normal trajectories of a particle superimposed . . . . .	40
4.7	Trajectories of a particle starting from different initial conditions in the 4 dimensional phase space . . . . .	41
4.8	Eigen vectors of relative velocity . . . . .	42

4.9 Relative Velocities of a particle starting from different initial conditions  
in the 4 dimensional phase space . . . . . 43

# Chapter 1

## Introduction

### 1.1 Background

To study advection of fluid tracer particles, one can either take the Eulerian approach or the Lagrangian approach. In the Lagrangian approach to advection we encounter differential equations of the form

$$\frac{dx}{dt} = u(x, y, t); \frac{dy}{dt} = v(x, y, t)$$

called Lagrangian advection equations. In an important paper published in 1984 by Hassan Aref[2], he demonstrated the practical importance of chaotic trajectories exhibited by such equations (even when the Eulerian flow field does not exhibit any chaotic behavior) in his work on fluid mixing, and he called this chaotic behavior of Lagrangian trajectories "Chaotic Advection". He demonstrated the application of chaotic advection to fluid mixing problems using the blinking vortex system which he introduced as a simple approximation of an agitator. The blinking vortex system is a system of point vortices which switch on and off between a fixed value of circulation

and zero periodically.

In this thesis however, we study the dynamics of spherical particles with finite size and mass as opposed to fluid tracers. This is of considerable interest, because the dynamics of such particles differ from that of the under-lying fluid flow [3]. This departure from fluid tracer behavior because of the inertia of such particles, leads to interesting behavior of the particles such as clustering and segregation in the presence of vorticity in the flow field. This clustering and segregation behavior is widely seen in both, natural flows and the flows in Industrial applications.

Over the years, many researchers have worked on studying the flow past a rigid sphere[4, 7, 20, 9], however, a comprehensive investigation of the equation of motion for a rigid spherical particle in a fluid was performed by Maxey and Riley [18] which eliminated some errors that existed in the body of work in this area and presented an updated version of the equation which is now called the Maxey-Riley equation named after the authors.

## 1.2 Motivation

There exist several reasons why studying the dynamics of inertial particles in the presence of vorticity is of great interest. Manipulating particle trajectories and controlling the eventual fate of particles so as to obtain size based segregation of particles finds numerous applications such as in microfluidic devices or industrial flows where impurities often manifest themselves in the form of particulate matter. While there exist several established methods for particle segregation, such as using mechanical means or using external electric or magnetic fields, these approaches impose limitations on the size and nature of the particles that can be controlled. For instance, using membrane filters to separate microparticles is limited by pore size and

the usage of external fields require the particles to be sensitive to the type of external field employed and in addition these external forces may damage sensitive biological cells which often are the kind of particles whose trajectory needs to be controlled [5]. These methods also depend on the scale of the process being undertaken as many of these processes can only be performed on small scale flows. In recent years, researchers have been focusing on purely hydrodynamic means to manipulate and control inertial particle motion as a way to overcome the limitations associated with the other methods[5, 6, 8, 17]. These methods often include modifying the flow geometry as a means to influence the hydrodynamic forces at play, however control strategies that can be dynamically varied and do not depend on the fixed flow geometry have obvious advantages over such methods.

Vorticity is an extremely important characteristic of fluid flow. Vortices are considered to be "The sinews and muscles of fluid motions" [Küchemann(1965)] as quoted in [21],(p.ix). Vortices are present not only in turbulent flows but are also seen in laminar flows in micro-channels. This gives us a very strong reason to study the interaction of inertial particles with vortices as a means to control the dynamics of inertial particles.

We now demonstrate two sample cases of flows with inertial particles in a vortex flow field.

### **1.2.1 Streaming Cell Flows**

As mentioned above, many of the inertial particle manipulation techniques are often applicable to small scale flows. One method which can be applied on a large scale is the use of streaming flow. Streaming cells can be created by the use of a circular cylinder executing small amplitude oscillations in a fluid [10].

Kwitae Chong et al[10] improved upon the expression for the flow generated by a circular cylinder in an oscillatory free stream which was obtained by Holtmark et al[14]. Switching the coordinates such that the cylinder is in oscillation in an otherwise stationary fluid, they showed that a cylinder undergoing sinusoidal oscillations along the horizontal axis such that,  $X(t) = A\sin(\omega t)$  where  $A$ , is the small amplitude of oscillation and  $\omega$  is the angular frequency of oscillation, produces four streaming cells. Figure(1.1) shows an image of streaming cells produced by an oscillating cylinder with a qualitative topology similar to that calculated by [10] and [14].

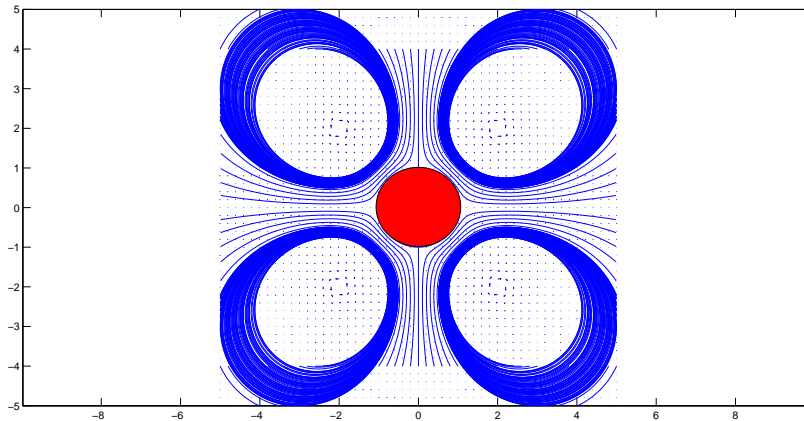


Figure 1.1: Vibrating cylinder in stationary fluid,  $x(t) = A\sin(\omega t)$

The study of inertial particles in a domain with four vortices, which is the first of two cases investigated in this work, is motivated by the application of cellular streaming flows to inertial particle manipulation.

### 1.2.2 Microfluidic Channel Flows

Microfluidics is an inter-disciplinary field of engineering where the behavior of fluid flow at micro scale is studied. This study of micro scale flow phenomenon with the eventual goal of its manipulation and control has gained momentum over

the last two decades owing to numerous applications it has found, such as in lab on chip devices, micro or nano-manufacturing and biofluid flows.

Microfluidic flow is most often studied with the intent of understanding the flow through microfluidic channels. Microfluidic channel design varies considerably from application to application. A range of different cross sections such as circular, square and rectangular and different channel geometries such as spiral, serpentine and straight channel geometries have been used in microfluidic studies[12, 8, 5, 6]

Inertial particles in microfluidic channel flows are encountered in applications such as particle sorting, particle filtering and particle encapsulation. The dynamics of inertial particles in such flows are manipulated using both active and passive methods. Active methods include the use of physical filters or the use of external fields such as electric or magnetic fields. In the case of passive methods, the hydrodynamic forces are manipulated with the goal of achieving controlled motion of the inertial particle. The hydrodynamic forces at play usually include lift forces and stokes drag force, but in the case of a curved microfluidic channel, an additional type of drag force comes into play due to the creation of dean vortices in the channel's cross section[11]. Thus, it is the balance of all these forces which cause particles to migrate across streamlines and settle down into focused bands whose relative position in the channel is a function of various parameters including the fluid and particle reynolds numbers, particle stokes number and dean number[22].

An experimental demonstration of this focusing behavior of particles in microfluidic channels was performed and it is seen that for any given Reynolds number, particles with a larger stokes number have a greater tendency to focus into thin bands in the channel. Figure(1.2).

The force balance on an inertial particle in the case of straight channels is quite well known, but in the case of curved channels, the presence of the dean vortices and



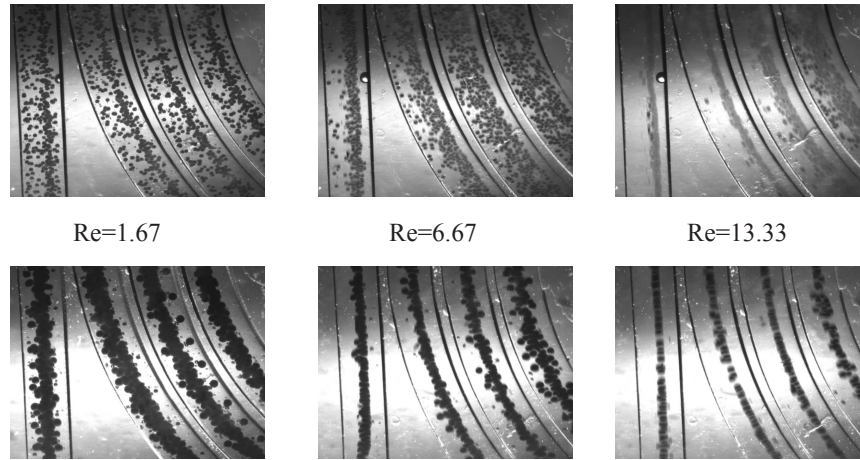


Figure 1.2: The top row shows particles of  $45\mu\text{ m}$  at various Reynolds numbers and the lower row shows the  $95\mu\text{ m}$  particles at the corresponding Reynold number, flowing through a curved channel

asymmetry in the axial velocity profile induced by the curvature of channel makes calculating the forces rather difficult and is not well established [22]. Thus, we seek to gain an understanding of how inertial particles interact with dean vortices in a confined microfluidic channel flow in the second case which is studied as part of this thesis, where the dynamics of inertial particles within a circular boundary for fluid flow is investigated.

### 1.3 Thesis Contributions

- The sensitivity of relative velocity of inertial particles to their spatial coordinates in a vortex flow field is studied.
- A method to separate and collect inertial particles based on stokes number using a simple four vortex flow configuration has been devised.

- Size based segregation of inertial particles using an array of oscillating cylinders is demonstrated.
- The mechanism of the focusing behavior of inertial particles in a curved microfluidic channel due to dean vortices generated in such channels has been demonstrated and stokes number dependence of particle focusing has been explained.
- Finally, a previously undocumented criteria to identify regions in phase space which enable inertial particles to lose their relative velocity has been observed and has been reported in this thesis.

## 1.4 Thesis Organization

The first chapter gives a historical background of the problem of studying chaotic trajectories of fluid tracers and Inertial particles. In particular the work of Maxey and Riley who carefully constructed the equations of motion for a rigid, spherical particle in a fluid is discussed. It also includes a description of the factors that motivated our investigation of inertial particle dynamics in the presence of vortex flow fields. Here, two examples of typical flows encountered in Industrial applications is discussed to further emphasize the importance of the problem being investigated. This is followed by a brief discussion of the contributions of this thesis to the existing literature.

The second chapter conducts a review of the theoretical background of point vortex dynamics and an expression for the velocity field generated by point vortices is derived. In addition, the theoretical background of inertial particle dynamics are reviewed and the governing equation of motion for a rigid, spherical particle in a fluid

is derived.

In the third chapter, the computational scheme used for the simulation of inertial particle dynamics is briefly discussed followed by a description of the simulation domain set up for both the cases investigated in this thesis.

Finally, the results from this study are presented and discussed in the final chapter. Some suggestions on future directions in research based on the conclusions are also presented.

# Chapter 2

## Review of Theory

### 2.1 Review Of Point Vortex Dynamics

The study of point vortices originated with the seminal work published by Helmholtz in 1858 in his paper called "Über Integrale der hydrodynamischen Gleichungen, welche den wirbelbewegungen entsprechen"[13] which was translated by Tait in 1867 as "On integrals of the hydrodynamical equations, which express vortex-motion". In this paper, Helmholtz introduces the point-vortex model where he imagines the vorticity of a fluid in 2D being confined to one or several isolated points which have an invariant amount of circulation( $\gamma$ ) associated with them. Now, we can imagine a 2D flow field with finite vorticity to be an ir-rotational flow field with Dirac delta functions of vorticity called point vortices distributed in it and the net vorticity can be written as a sum of the point vortices[23].

$$\omega = \sum_{k=1}^n \gamma_k \delta(z - z_k)$$

$$\delta(z - z_k) = \gamma, \text{ if } z = z_k$$

$$\delta(z - z_k) = 0, \text{ if } z \neq z_k \quad (2.1)$$

The 2D approximation of fluid flow is valid for cases where flow field does not vary to an appreciable extent in the third dimension or when the third dimension is very small compared to the first two dimensions[23].

Vorticity is defined as the curl of the fluid velocity.

$$\omega(z, t) = \nabla \times v(z, t) \quad (2.2)$$

where v is the velocity of the fluid

Helmholtz realized that like the velocity field, the vorticity field can often hold very important information about the nature of the flow[23].

Starting with the Incompressible Navier-Stokes Equations for an in-viscid fluid, also called the Euler Equations

$$\frac{\partial u}{\partial t} + u \cdot \nabla u = -\frac{\partial p}{\partial x}$$

$$\nabla \cdot u = 0 \quad (2.3)$$

We obtain the vorticity transport equation in 2D by taking the curl of equation(2.3). Working with two dimensions avoids the critical vortex-stretching and bending term

which makes solving the vorticity transport equations analytically intractable.

$$\begin{aligned}\frac{\partial w}{\partial t} + u \cdot \nabla w &= 0 \\ \nabla \cdot w &= 0\end{aligned}\tag{2.4}$$

This can also be written using the material derivative operator  $\frac{D()}{Dt} = \frac{\partial}{\partial t} + u \cdot \nabla()$  as

$$\frac{Dw}{Dt} = 0\tag{2.5}$$

Thus, for the case of Inviscid, Barotropic, 2D flows with only conservative body forces the total vorticity is conserved along a streamline and we understand that as the vortices move through a fluid the velocity field around them gets modified by their presence and in turn the local velocity advects the point vortices to a new position(provided they are free to move) but their net circulation strength is not modified.

### 2.1.1 Velocity Field Due To Point Vortices

Because in-compressible fluid is being considered, ( $\frac{\partial u}{\partial x} + \frac{\partial v}{\partial y} = 0$ ), the existence of a stream function  $\psi$  is assured and it is by definition related to velocity as[15]

$$\begin{aligned}u &= \frac{\partial \psi}{\partial y} \\ v &= -\frac{\partial \psi}{\partial x}\end{aligned}\tag{2.6}$$

To obtain an expression for the velocity field due to the point vortices, we shall first perform a procedure called Helmholtz or Hodge decomposition where the

velocity is decomposed into a divergence free solenoidal vector potential ( $\psi$ ), which is the same as the stream function, and a curl free vector potential ( $\phi$ ), see (Lamb,1932)

$$\begin{aligned} u &= u_w + u_\phi \\ (or)u &= \nabla \times \psi + \nabla\phi \end{aligned} \tag{2.7}$$

From the definition of vorticity  $\omega = \nabla \times u$  and using the identity  $\nabla \times \nabla \times \vec{u} = \nabla(\nabla \cdot \vec{u}) - \nabla^2\vec{u}$  we find that the stream-function is related to the vorticity by the Poisson equation

$$-\omega = \nabla^2\psi \tag{2.8}$$

We know that the vorticity can be expressed as a sum of Dirac Delta functions(2.1), thus , the solution to (2.8) can be expressed in terms of the Green's function  $G(x)$  [19]

$$\psi(z) = \int G(z - z_k)w(z)dz, \tag{2.9}$$

where,

$$\mathcal{L}G(z - z_k) = \delta(z - z_k), \tag{2.10}$$

$$G(x) = \begin{cases} -\frac{1}{2\pi}\log\|X\|, & \text{in } R^2 \\ \frac{1}{4\pi}\frac{1}{\|X\|}, & \text{in } R^3 \end{cases}$$

is the Green's function in free space for linear operator  $\mathcal{L} = \nabla^2$  which is the Laplace operator[19].

From this we determine the stream function for the flow field can be expressed as

$$\psi = -\frac{\sum_{k=1}^n \gamma_k}{2\pi} \log|z - z_k| \quad (2.11)$$

And thus the x and y component of the velocity can be obtained by differentiating the velocity field as per the definition of the stream function.

$$\begin{aligned} \dot{x} &= -\frac{\sum_{k=1}^n \gamma_k}{2\pi} \frac{(y - y_k)}{|z - z_k|^2} \\ \dot{y} &= \frac{\sum_{k=1}^n \gamma_k}{2\pi} \frac{(x - x_k)}{|z - z_k|^2} \end{aligned} \quad (2.12)$$

The velocity fields generated by simple vortex flow configurations have been shown in Figures 2.1 and 2.2.

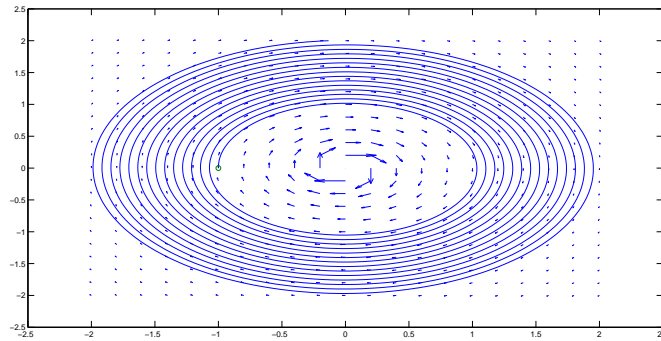


Figure 2.1: Velocity field generated by a single vortex at the origin

## 2.2 Other Approximate Models Of Vorticity

The point vortex model is an approximation used for ease of representing vorticity in fluid flows. It enables us to model vorticity as isolated distributions of



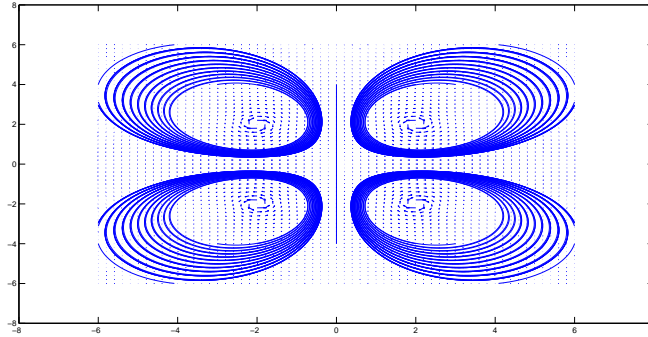


Figure 2.2: Velocity field generated by a four vortex configuration

circulation which get advected by the underlying fluid flow. However, this model implies the existence of singularities in the velocity field at the center of the point vortex. To avoid this, and to make the velocity field more realistic, we could adopt one of the following approximate models of vorticity.

### 2.2.1 Rankine Vortex

A Rankine vortex is a simple model of a point vortex where the vorticity is non-zero and constant( $\omega_0$ ) inside a fixed core of radius ' $R_c$ ' and for any radius  $R > R_c$  a vorticity jump from  $\omega_0$  to 0 takes place[15]. This model helps us avoid the singular velocity field associated with the ideal point vortex. The velocity inside the vortex core is thus governed by a modified form of equations(2.12) given by,

$$\begin{aligned} \dot{x} &= -\frac{\sum_{k=1}^n \gamma_k (y - y_k)}{2\pi R_c^2} \\ \dot{y} &= \frac{\sum_{k=1}^n \gamma_k (x - x_k)}{2\pi R_c^2} \end{aligned} \quad (2.13)$$

the velocity is governed by equations(2.12) outside the Rankine core. The velocity profile of a Rankine vortex is as shown in Figure(2.3).

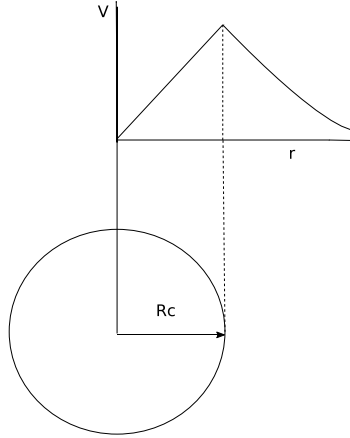


Figure 2.3: Velocity profile of a rankine vortex

### 2.2.2 Use Of A Regularization Parameter

The use of a regularization model ' $\delta$ ' is one way of modeling the viscosity in a fluid with vorticity. Using a small value of ' $\delta$ ' such that ' $\delta^2$ ' is very small will ensure that the problem of infinite velocities at the vortex center in a point vortex is avoided, and at the same time a weak viscous effect in the fluid is incorporated. This will of course, take away some advantages of using the ideal point vortex model such as the ability to consider the fluid inviscid and thus being able to use ideas such as the Milne-Thomson Circle theorem(section(2.3)) to model a transport barrier to fluid flow. The velocity field of a regularized point vortex would thus be,

$$\begin{aligned}
\dot{x} &= -\frac{\sum_{k=1}^n \gamma_k}{2\pi} \frac{(y - y_k)}{|z - z_k|^2 + \delta^2} \\
\dot{y} &= \frac{\sum_{k=1}^n \gamma_k}{2\pi} \frac{(x - x_k)}{|z - z_k|^2 + \delta^2}
\end{aligned} \tag{2.14}$$

### 2.2.3 Lamb-Oseen Vortex

The Lamb-Oseen vortex is one of the simplest examples of a viscous vortex and it is a more realistic model of viscosity than the use of a regularization parameter. Unlike the rankine vortex where the vorticity is constant inside its core, the vorticity of a Lamb-Oseen vortex is a function of the distance from vortex center 'r' and time 't'. The effect of viscosity in this type of vortex is to slowly smudge an ideal point vortex which is a line vortex in three dimensions into a Gaussian, asymptotically with time [23]. Thus the velocity due a Lamb-Oseen vortices would now be governed by the set of equations,[21]

$$\begin{aligned}
\dot{x} &= -\frac{\sum_{k=1}^n \gamma_k (1 - e^{-\frac{((x-x_k)^2 + (y-y_k)^2)}{R_c^2}}))}{2\pi} \frac{(y - y_k)}{|z - z_k|^2} \\
\dot{y} &= \frac{\sum_{k=1}^n \gamma_k (1 - e^{-\frac{((x-x_k)^2 + (y-y_k)^2)}{R_c^2}}))}{2\pi} \frac{(x - x_k)}{|z - z_k|^2}
\end{aligned} \tag{2.15}$$

Where  $R_c$  is the core radius and the resulting core velocity profile is as shown in Figure(2.4).

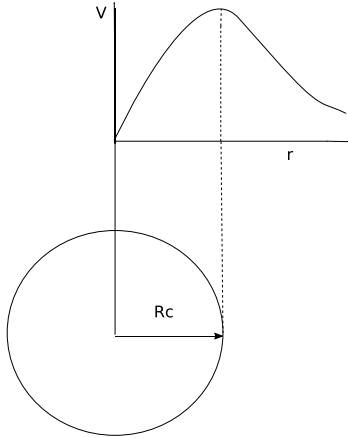


Figure 2.4: Velocity profile of a Lamb-Oseen vortex

## 2.3 Milne Thomson Circle Theorem

The Milne-Thomson Circle theorem provides us with a useful technique when modeling fluid flows to modify the interior boundary conditions by introducing a circular cylinder into the domain. The statement of the proof is thus[16]:

**Circle Theorem.** *Let there be irrotational two-dimensional flow of incompressible inviscid fluid in the  $z$  plane. Let there be no rigid boundaries and let the complex potential for the flow be  $f(z)$ , where the singularities of  $f(z)$  are all at a distance greater than ' $a$ ' from the origin. If a circular cylinder, typified by its cross-section the circle  $C, |z| = a$ , be introduced into the field of flow, the complex potential becomes*

$$w = f(z) + \bar{f}\left(\frac{a^2}{z}\right) \quad (2.16)$$

This has been demonstrated in Figures (2.5) and (2.6) where the first image corresponds to the streamlines of a normal two vortex flow field and the second image has a circular cylinder imposed upon the flow field by the introduction of two image vortices placed such that the Milne-Thomson Circle theorem is satisfied.

This idea can be used to impose a circular transport barrier on the fluid when

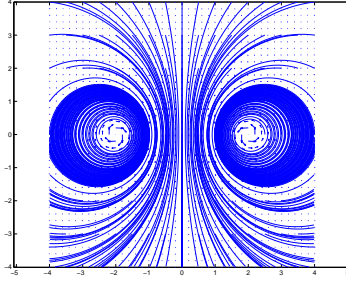


Figure 2.5: Streamlines of a 2-vortex flow

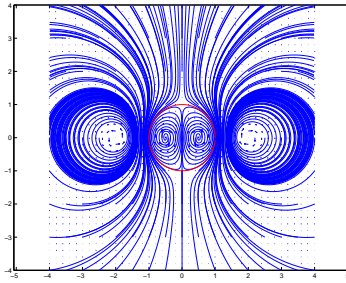


Figure 2.6: Stream lines of a 2-vortex flow with cylinder

we model microfluidic flows in a confined channel.

## 2.4 Review Of Inertial Particle Flows

Tchen [9] extended the work of Basset[4], Boussinesq[7] and Oseen[20] on the settling on particles under gravitational forces in a still fluid to the case of particle motion in an unsteady but uniform flow field. He then tried to extend this to the case of an unsteady and un-uniform flow. This second extension was modified and corrected by several researchers. The form of the equation of motion for small, spherical, rigid tracer in incompressible fluid which is most widely used is the one proposed by Maxey-Riley [18] called the Maxey-Riley equation.

$$\begin{aligned} \rho_p \frac{dv}{dt} = & \rho_f \frac{Du}{Dt} + (\rho_p - \rho_f)g - \frac{9\nu\rho_f}{2a^2} \left( v - u - \frac{a^2 \nabla^2 u}{6} \right) \\ & - \frac{\rho_f}{2} \left( \frac{dv}{dt} - \frac{D}{Dt} \left[ u + \frac{a^2 \nabla^2 u}{10} \right] \right) - \frac{9\rho_f}{2a} \sqrt{\frac{\nu}{\pi}} \int_0^t \frac{1}{\sqrt{t-\tau}} \frac{d}{d\tau} \left( v - u - \frac{a^2 \nabla^2 u}{6} \right) d\tau \end{aligned} \quad (2.17)$$

Here  $\rho_p$  and  $\rho_f$  are the densities of the particle and fluid respectively. 'v' is the particle velocity and 'u' is the velocity of the fluid at the location of the particle. 'g' is the acceleration due to gravity,  $\nu$  is the kinematic viscosity and 'a' is the particle radius.

For the Equation(2.17) to be valid, the following assumptions need to hold true:

- $\frac{a}{L} \ll 1$ ,
- $\frac{a(v-u)}{\nu} \ll 1$ ,
- $\left(\frac{a^2}{\nu}\right)\left(\frac{U}{L}\right) \ll 1$ ,

where L and (U/L) are the length scale and velocity gradient scale for undisturbed fluid flow.

That is, the particle radius and particle reynold' s number are small and so are the velocity gradients around it.

The first term on the right hand side is the force exerted on the particle by the undisturbed flow. The second term is the buoyancy force and the third is the stokes drag. The fourth term is the added mass correction and the final term is the Basset-Boussinesq history force.

The Stokes drag is the dominant term in this equation and very often the inertial particle flow reduces to a stokes flow, however there are cases where other terms of this equation can become significant, for instance if the particle is accelerating with time very fast, the Basset-Boussinesq history force becomes significant and the Basset-Boussinesq history force is also significant in flows where the particle is bound to revisit the same location several times in a short time span, such as in oscillatory flows[18]. The buoyancy force is present if the particles are not of neutral density.

We shall now derive the simplified form of Eq(2.17) using the procedure outlined in [18].

The particle radius 'a' is chosen such that it is not negligible, however the square of 'a' is a sufficiently small quantity compared to the characteristic length scale of the flow (L) that the Faxen correction term  $a^2\nabla^2u$  can be neglected. The Basset history term which includes viscous memory effects into the equation is time and memory consuming and is usually neglected when restricting ourselves to neutrally buoyant particles ,i.e.,  $\rho_p = \rho_f$  . Thus, using these assumptions and approximations equation (2.17) can be simplified as

$$\rho \frac{dv}{dt} = \rho \frac{Du}{Dt} - \frac{9\nu\rho}{2a^2}(v - u) - \frac{\rho}{2}\left(\frac{dv}{dt} - \frac{Du}{Dt}\right) \quad (2.18)$$

The derivative

$$\frac{Du}{Dt} = \frac{\partial u}{\partial t} + (u \cdot \nabla)u \quad (2.19)$$

is defined along the path of a fluid element whereas the derivative  $\frac{du}{dt}$  is defined along the trajectory of the inertial particle.

$$\frac{du}{dt} = \frac{\partial u}{\partial t} + (v \cdot \nabla)u \quad (2.20)$$

If we assume that for very small neutrally buoyant particles  $\frac{Du}{Dt} = \frac{du}{dt}$  is a valid approximation, then equation (2.18) can be re-written as

$$\frac{dw}{dt} = -\frac{2}{3}St^{-1}w \quad (2.21)$$

Where St is the particle Stokes number  $St = 2a^2U/(9\nu L) = (\frac{2}{9})(\frac{a}{L})^2 Re_f$ , and  $Re_f$  is the fluid Reynolds number and  $w = (v - u)$ .

Which upon solution yields

$$w = w_0 e^{-\frac{2}{3}St^{-1}t} \quad (2.22)$$

This essentially means that if the inertial particles are released with a finite relative velocity  $w_0$ , the relative velocity decays exponentially to zero with time 't' and we would essentially be integrating fluid tracers. However, we know that this is not the case and that even for very small inertia, the particles exhibit dynamics which are very different from that of fluid tracers. Thus,  $\frac{Du}{Dt} \neq \frac{du}{dt}$  and we need to include the expressions [2.19] and [2.20] into equations [2.18] to re-write it as

$$\frac{d(v-u)}{dt} = -[(v-u) \cdot \nabla]u - \frac{2}{3}St^{-1}(v-u) \quad (2.23)$$

(or)

$$\frac{dw}{dt} = -(J + \mu I) \cdot w \quad (2.24)$$

Where, J is the gradient of undisturbed velocity field of the fluid which for the two dimensional flow being considered in this case is the jacobian

$$J = \begin{pmatrix} \partial_x u_x & \partial_y u_x \\ \partial_x u_y & \partial_y u_y \end{pmatrix}. \text{ w is (v-u) and } \mu \text{ is } \frac{2}{3}St^{-1}$$

Now, to obtain the criteria for making sure that the dynamics of inertial



particles are sufficiently different from that of tracer particles, we diagonalize  $J$  and in the process obtain the diagonalized version of (2.24)

$$\frac{dw_d}{dt} = \begin{pmatrix} \lambda - \frac{2}{3}St^{-1} & 0 \\ 0 & -\lambda - \frac{2}{3}St^{-1} \end{pmatrix} \cdot wd \quad (2.25)$$

Now, as it is clear from the above equation, the criteria we are looking for is the parameter  $Re(\lambda) - \frac{2}{3}St^{-1}$ . If this parameter is positive, then the initial relative velocity  $w_0$  assigned to the particles may grow exponentially and will definitely not go to zero very fast.

Thus, the system of equations

$$\frac{dr}{dt} = w + u \quad (2.26)$$

where  $r(x, y)$  is the particle position, and equation (2.24) form a non-linear dynamical system with a 4 dimensional phase space  $\xi = (x, y, w_x, w_y)$  and can be represented as

$$\frac{d\xi}{dt} = F(\xi) \quad (2.27)$$

# Chapter 3

## Computational Methodology

### 3.1 Runge-Kutta Fourth Order Scheme

To numerically integrate the four dimensional system defined in Eq(2.27), we use a Runge-Kutta, fourth order, non-stiff differential equation solver which takes in initial values of the four variables in this 4 dimensional dynamical system and integrates over a specified time interval to return the position and relative velocities after regular intervals in time. The time intervals to store position and relative velocity data is given as input to the solver.

### 3.2 Four Vortex Configuration

For the case of a four vortex flow we consider four vortices placed at the corners of a 4 x 4 square centered at the origin. The vortices have circulation strengths of equal magnitude, while the direction of rotation is anti-clockwise for vortices in the first and third quadrant and clockwise in second and fourth quadrants. The procedure for choosing the right circulation strength has been described in section(4.1.1). A

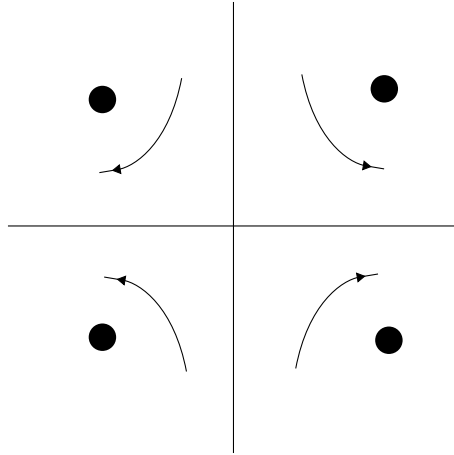


Figure 3.1: The four vortex configuration used to investigate particle trapping using vibrating cylinders

schematic of this configuration of flow has been shown in Figure(3.1)

### 3.3 Particles In a Confined Geometry

Two dean vortices are formed in flows through curved microfluidic channels. Hence, we consider two vortices, one above and one below the  $y=0$  line at  $(0.5,0.5)$  and  $(0.5,-0.5)$  on a 2D plane. To simulate the confined geometry of a microfluidic channel with a circular cross section, we use the Milne Thomson circle theorem described in section (2.3) and place two image vortices at  $(1,1)$  and  $(1,-1)$  of circulation that is opposite in direction to those at  $(0.5,0.5)$  and  $(0.5,-0.5)$  respectively. This gives us a circular boundary of radius 1 for fluid flow. As mentioned, this boundary is a transport barrier only for fluid flow and does nothing to stop the particles from moving out of the boundary. Particles come into contact with the channel walls in real flows as there is no mechanism that prevents this, hence we reflect particles off the walls of our circular boundary if they come into contact with the walls of the channel. This is achieved by using the MATLAB event function for ODE solvers which can be used

to detect particular events during the course of numerical integration. The specific event of interest here is the particle coming in contact with the boundary walls which are a fixed distance from the origin. We assume that the particles undergo perfectly elastic collisions and we also consider the vorticity generated by particles bouncing off the boundary walls [1] to be extremely small compared to the strength of dean vortices and do not influence the dynamics of the particles appreciably. Thus, the velocity vector striking the boundary wall at an angle  $\theta$  to the normal is rotated such that it is reflected back into the channel at the same angle, using the simple identity given by  $w = v - 2(v \cdot \hat{n})\hat{n}$ . Vector  $w$  and  $v$  are sketched in Figure(3.2).

Thus, using this method, we can now make sure that particles do not escape the circular boundary. An example of a single particle driven by dean vortices bouncing off the walls has been shown in Figure(3.3)

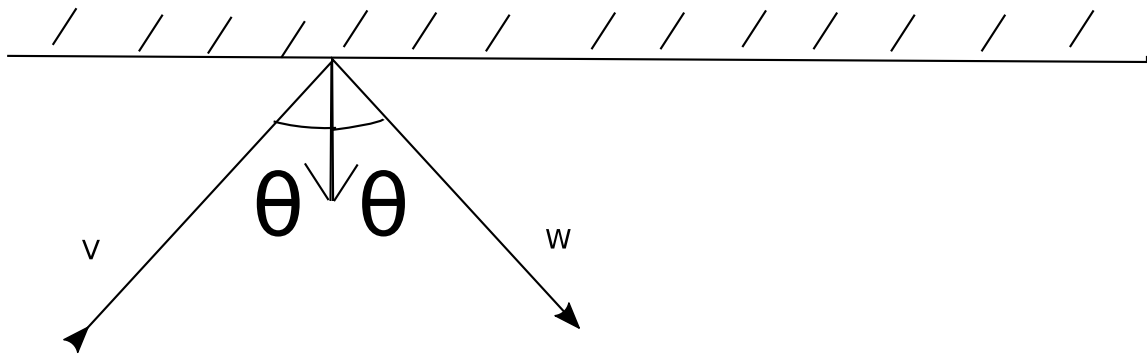


Figure 3.2: Vector  $w$  is the reflected vector and  $v$  is the incident vector related by  $w = v - 2(v \cdot \hat{n})\hat{n}$

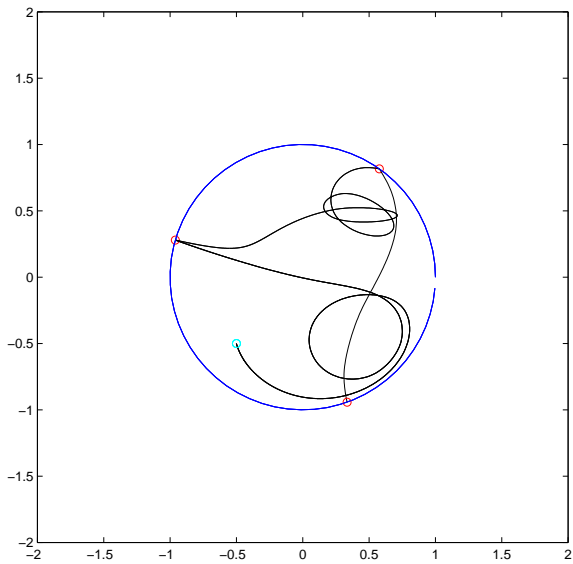


Figure 3.3: Trajectory of a particle reflecting off boundary walls

# Chapter 4

## Results and Discussion

Here, we present the results of our numerical investigation of the dynamics of inertial particles in simple vortex flow configurations. The criteria to ensure that relative velocity imparted to inertial particles initially does not die out exponentially fast, has been outlined. The criteria is in the form of a spatial set in the vicinity of the vortices which can be computed from the velocity gradient information of the flow field, within which the particle velocity relative to the fluid does not go to zero.

In the first case, the Maxey-Riley equations[18] were numerically integrated for particles in a four vortex flow configuration. This model is then further developed to include an array of several vortices that can be used to segregate particles by size.

In the second case, the inertial particle dynamics is simulated in a confined geometry to study the phenomenon of inertial particle focusing in curved micro-channels in the presence of dean vortices. Stokes number dependence for focusing has been demonstrated.

We also introduce a new mechanism by which an inertial particle can lose its velocity relative to the ambient flow and can act as a mere fluid tracer under certain conditions.

## 4.1 Sensitivity Field Of Relative Velocity

In almost all naturally occurring flows, inertial particles have a certain velocity relative to the ambient fluid. The source of this relative velocity could be any number of external factors ranging from vibration of the system to the sudden start of fluid flow, which has the effect of imparting a velocity to the particles different from that of the fluid, because of the particle's inertia.

If the relative velocity imparted to a certain particle decays to zero exponentially in time, we would not observe any difference in the dynamics of different sized particles, and all of them would follow the streamlines of flow. However, for every flow field, there exist regions of the domain inside which the relative velocity of the inertial particle does not decay to zero. The profile of this region varies with stokes number of the particle and the circulation strength of the flow. To be able to identify these regions of interest, we need to go back to the equations derived in section(2.4)

The gradient of velocity field at any given point in the domain is given by the Jacobian of the velocity field in 2D  $J = \begin{pmatrix} \partial_x u_x & \partial_y u_x \\ \partial_x u_y & \partial_y u_y \end{pmatrix}$ . From equation (2.24) we know that the rate at which the relative velocity ( $w$ ) changes is described as

$$\frac{dw}{dt} = -(J + \mu I) \cdot w \quad (4.1)$$

diagonalizing this equation yields the following relationship between the rate of change of  $w$ , the stokes number and the eigen values of the velocity gradient at that point in the domain.

$$\frac{dw_d}{dt} = \begin{pmatrix} \lambda - \frac{2}{3}St^{-1} & 0 \\ 0 & -\lambda - \frac{2}{3}St^{-1} \end{pmatrix} \cdot w_d \quad (4.2)$$

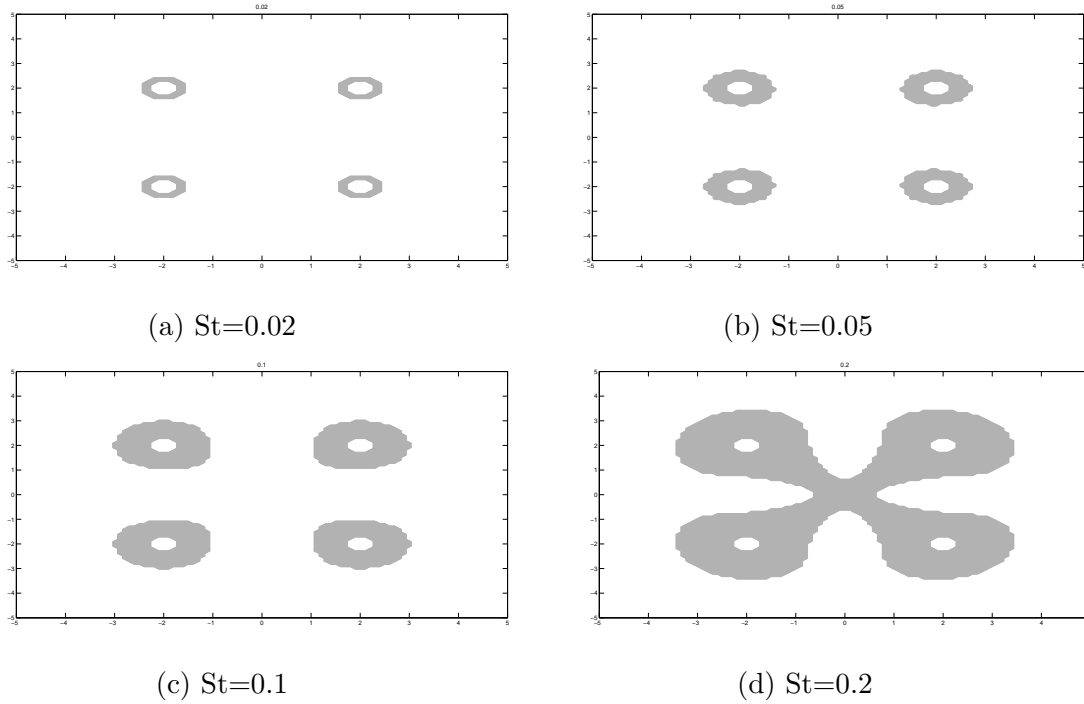


Figure 4.1: Binary plots of regions with  $Re(\lambda) - \frac{2}{3St} > 0$  in gray and  $Re(\lambda) - \frac{2}{3St} < 0$  in white for various Stokes numbers

Thus, if the particles with a certain relative velocity start off from or move through a region with the parameter  $Re(\lambda) - \frac{2}{3St} > 0$ , this ensures that atleast one of the two components of relative velocity in the 2D plane, grows with time. However, if the particles enter a region with a negative value for the parameter  $Re(\lambda) - \frac{2}{3St}$ , the relative velocity decays quickly and the particles start moving with the streamlines of flow.

Binary plots of the sensitivity field for the case of a four vortex flow has been shown in Figure(4.1). The regions with a positive value of parameter  $Re(\lambda) - \frac{2}{3St}$  have been shaded gray, whereas the regions with negative values for  $Re(\lambda) - \frac{2}{3St}$  have been shaded white. For a larger Stokes number, the value of the parameter  $\frac{2}{3St}$  is smaller and thus the gray region is larger in plots for particles with greater Stokes numbers for any given Reynolds number of the flow.



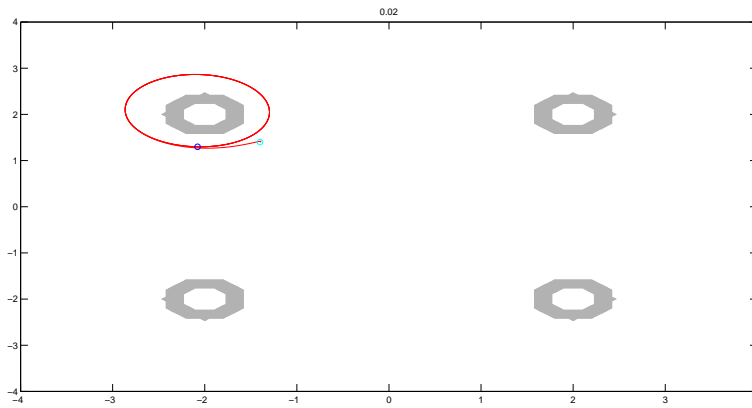
### 4.1.1 Separation Of Particles By Stokes Number

Increasing the circulation strength of the vortices and thereby increasing Reynolds number of the flow, increases the size of the positive region for a given stokes number of the particles. Thus, using a careful combination of the particle stokes number and flow Reynolds number in addition to choosing the right configuration of vortices in the plane, we can design a system which acts as a particle repeller in some regions of flow and as an attractor for particles in other regions.

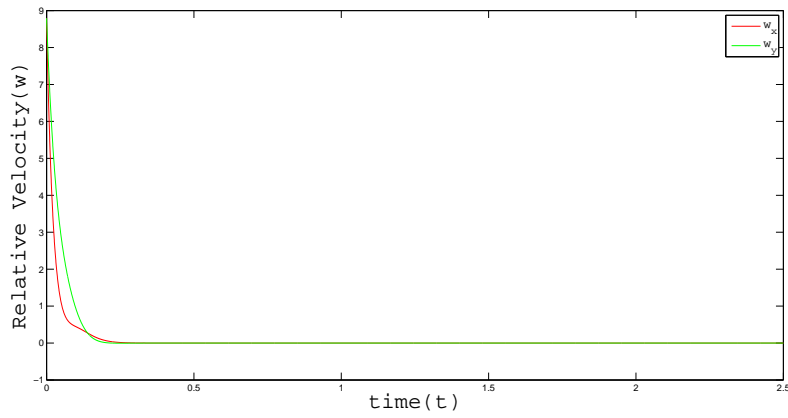
To demonstrate this, we choose a set of stokes numbers for a single particle starting with an initial relative velocity such that its velocity is directed at the nearest vortex in the second quadrant of the four vortex flow configuration. The value of circulation chosen for the vortices are such that the particle starts off inside the gray region of the binary plots for larger stokes numbers and in the white region for lower stokes numbers. The relative velocity sensitivity field so obtained is shown below in Figure(4.2).

Numerical integration of particle trajectory for Stokes number of 0.02 shows us that the relative velocity imparted dies down exponentially fast before the particle can enter the gray region, and the particle settles into a large periodic orbit along the streamlines around the vortex. For a larger stokes number such as the case of  $St=0.1$  or  $St=0.2$ , we see that unlike the case of small stokes number particles, their relative velocity sensitivity field has grown larger to include the initial position of the particle inside the gray region. This ensures that the particle's relative velocity does not go to zero and the particles cut across streamlines of flow until they reach the vortex and collapse into the core of the vortex where they lose all their relative velocity.

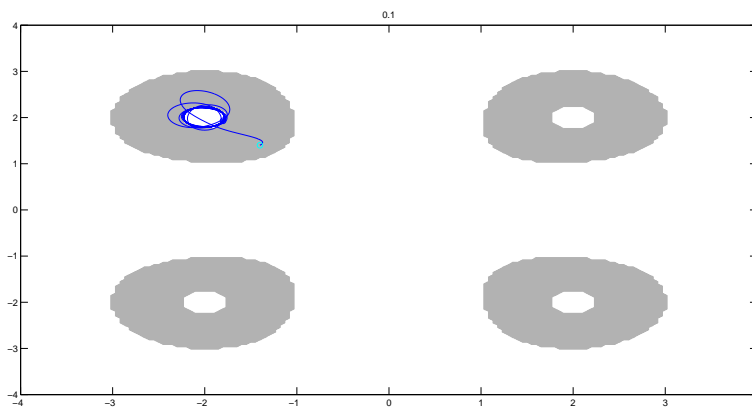
This can now be used to design particle traps which can selectively trap particles of particular sizes by exploiting the dynamics of inertial particles, rather than



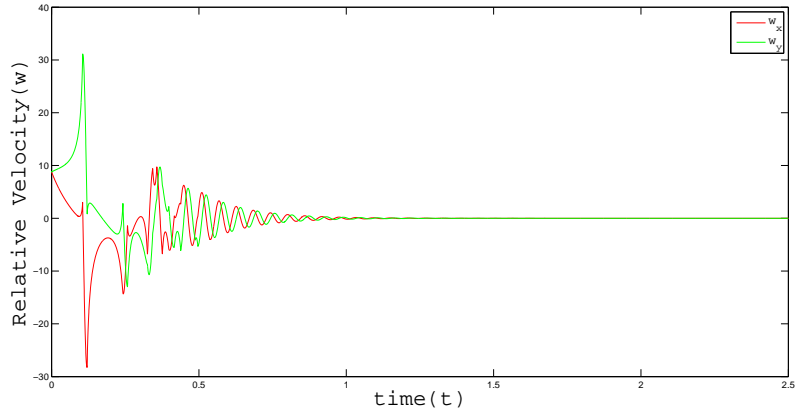
(a) Trajectory of a particle with  $St=0.02$



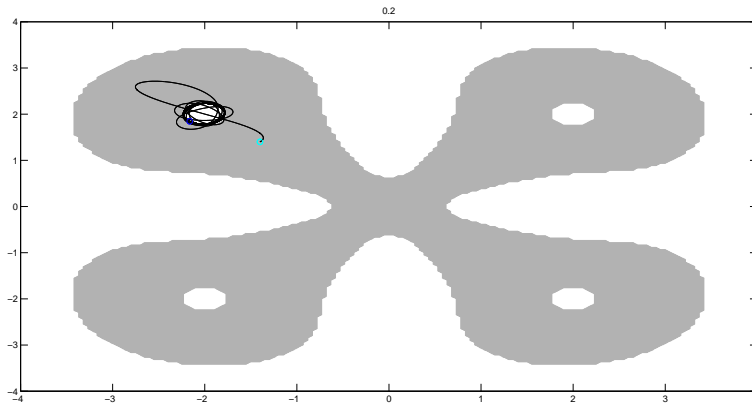
(b) Relative velocity of a particle with  $St=0.02$



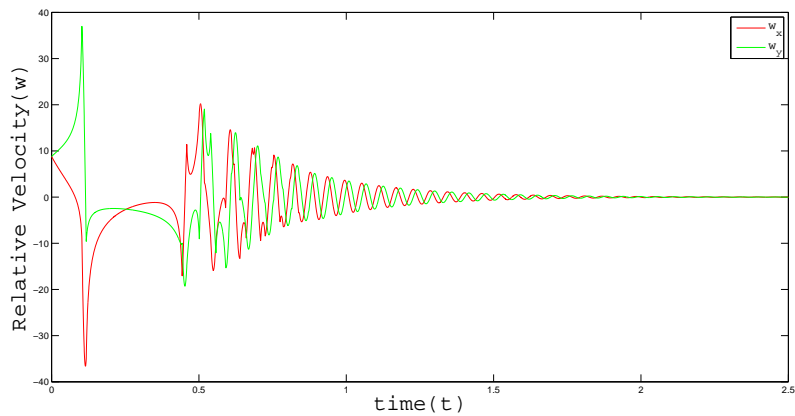
(c) Trajectory of a particle with  $St=0.1$



(d) Relative velocity of a particle with  $St=0.1$



(e) Trajectory of a particle with  $St=0.2$



(f) Relative velocity of a particle with  $St=0.2$

Figure 4.2: Particles of different stokes numbers settling down into periodic orbits of different radii around a vortex

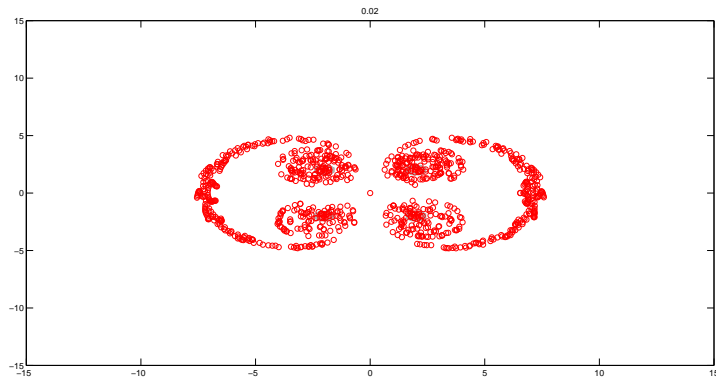
using external forces. One such mechanism is discussed next.

## 4.2 Size Based Segregation of Particles Using an Array of Oscillating Cylinders

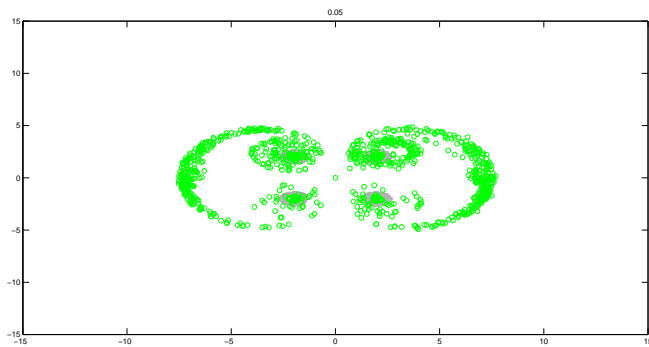
Here, we seek to separate particles by size by using the four vortex flow configuration introduced in section 2 of chapter 3. The motivation for using this configuration of vortices has been detailed in chapter 1, section 1.2.1, where the streaming cells set up by an oscillating cylinder is identified as a vortex generation mechanism which can be used in flows of larger scales.

A circulation strength has to be chosen for vortices such that a large number of the larger particles are captured at vortex cores while a lesser number of the smaller particles are captured. The appropriate circulation strength can be chosen by looking at the binary plots of the relative velocity sensitivity field introduced in section(4.1). For a simple four vortex configuration and a sample of approximately thousand particles, initially spread uniformly on a 3 X 3 rectangular grid, the position of the particles after a time 't' has been plotted in Figure(4.3).

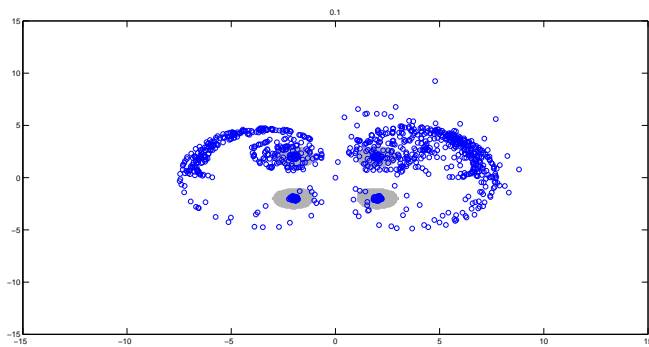
As seen here, many particles cluster around the vortex cores, but in addition to clustering inside of vortex cores, several particles do escape the cores and settle into regions outside of the repelling region of the sensitivity field. To overcome this loss of particles that we seek to separate by size, we use not one set of four vortices but a large number of similar four vortex cells which can be thought of as streaming cells generated by an array of oscillating cylinders as opposed to a single oscillating cylinder. This ensures, that particles which have escaped the vortex cores closest to their starting positions do not easily lose their relative velocities. This is especially



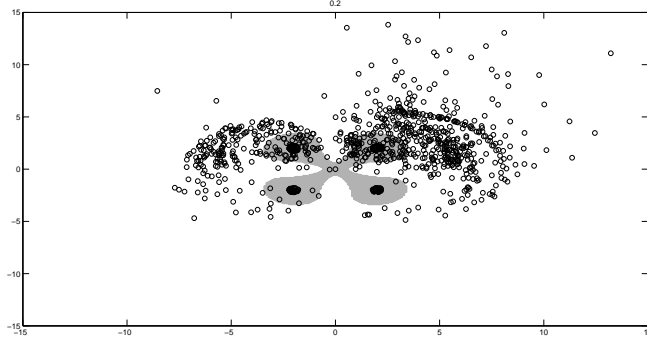
(a) Distribution of Particles of  $St=0.02$  in a four vortex flow



(b) Distribution of Particles of  $St=0.05$  in a four vortex flow



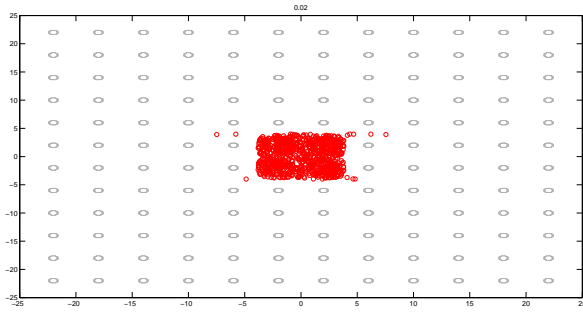
(c) Distribution of Particles of  $St=0.1$  in a four vortex flow



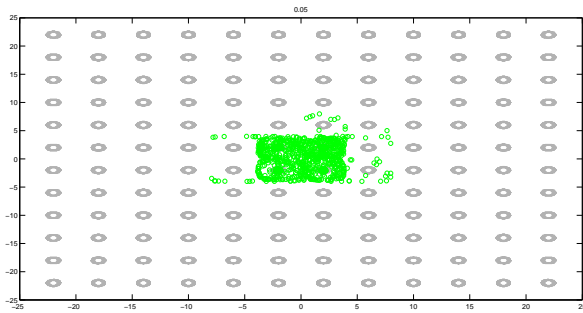
(d) Distribution of Particles of  $St=0.2$  in a four vortex flow

Figure 4.3: Particles of different sizes trapped at the vortex cores in a four vortex flow

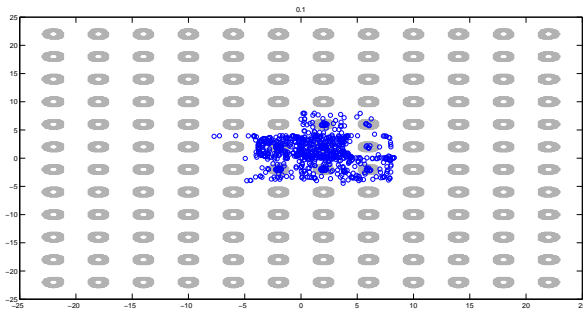
true for the particles with higher stokes numbers because the particles are more likely to always be in the vicinity of an unstable relative velocity region. Plots of a 12 X 12 or 144 vortex flow field for the same number of particles has been plotted Fig(4.4). The results from these plots show that a far greater number of particles have now been captured within vortex cores for the larger particles (about 25% for particles of  $St=0.1$  and a little more than 50% for  $St=0.2$ ) and the number of particles of smaller size ending up in the core region is comparatively very small (6.8 % for  $St=0.02$  and 13.6% for  $St=0.05$ ). Most systems in practice will not be isolated systems and have vibrations and other disturbances associated with them. Such ambient vibrations would serve as repeated perturbations to the particle relative velocity. This would ensure that an increasing number of particles which have settled into periodic orbits end up inside the vortex cores, eventually giving rise to almost 100% collection of larger particles, while for smaller particles small perturbations are not sufficient to cause them to fall into a sensitive relative velocity area and are consequently less likely to fall into the vortex cores. Hence, this is an effective method of trapping and separating large particles from smaller particles in flows.



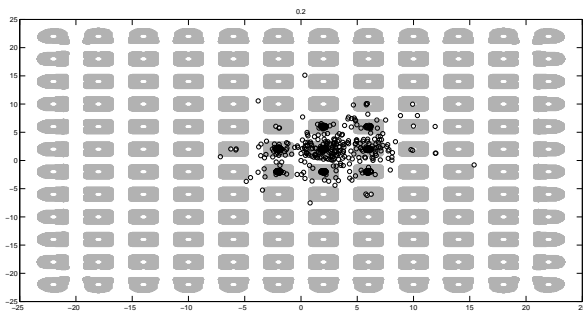
(a) Distribution of Particles of  $St=0.02$  in a vortex array



(b) Distribution of Particles of  $St=0.05$  in a vortex array



(c) Distribution of Particles of  $St=0.1$  in a vortex array



(d) Distribution of Particles of  $St=0.2$  in a vortex array

Figure 4.4: Distribution of particles of a range of stokes numbers in a vortex array

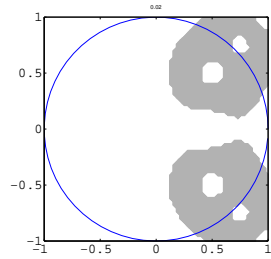
## 4.3 Inertial Particle Focusing In A Circular Cylinder

In this investigation, we seek to explain the differential focusing of inertial particles of different sizes in a confined micro-channel. We have used the Milne-Thomson circle theorem introduced in chapter 2 as explained in chapter 3 to impose a circular barrier to fluid flow. The assumptions under which this simulation has been performed, namely, Coefficient of restitution=1 for particle-wall collisions and ignoring the vortex flow generated by particles bouncing off channel walls, have been detailed in section 3.3. As it is observed experimentally Figure(1.2), the smallest particles are dispersed in the channel while the larger particles have a tendency to cluster around the vortex cores giving rise to the focused bands in microfluidic flow experiments. The reason for this behavior can be understood looking at the binary plots of the sensitivity field for this flow Figure(4.5(a,c,e,g)). Looking at these plots it is apparent that for stokes number 0.02, very few particles in the channel would be present in the repelling region, these particles alone may end up in the vortex core or they may simply migrate to the white non-repelling region outside the repelling zone. As these particles get larger, so do the repelling regions. This ensures that more and more particles end up clustered around the vortex core for higher stokes numbers because the particles can not exit the boundary imposed upon them.

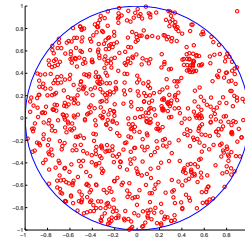
A simulation was performed for particles with stokes numbers 0.02,0.05,0.1 and 0.2 to clearly demonstrate this behavior of inertial particles in a confined geometry. The resulting simulation results are displayed in Figure(4.5(b,d,f,h)).

It is found that for particles of stokes number 0.2, 52% of the particles end up clustered in the vortex core region of small radius 0.1, where as the number is 49% for 0.1, 24% for 0.05 and only 5% for particles with stokes number 0.02. Vibration of

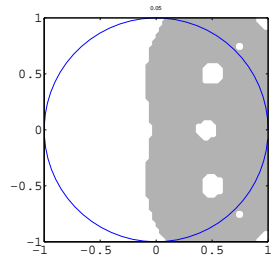




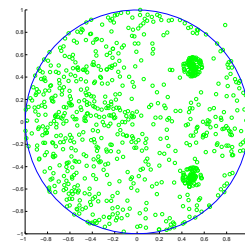
(a) Sensitivity field for  $St=0.02$



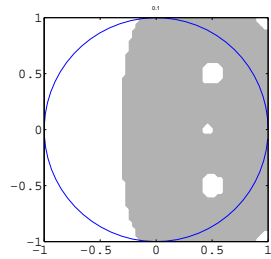
(b) Particles of  $St=0.02$  dispersed in a channel



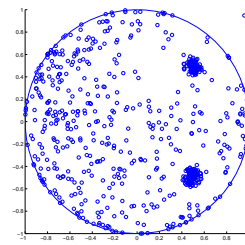
(c) Sensitivity field for  $St=0.05$



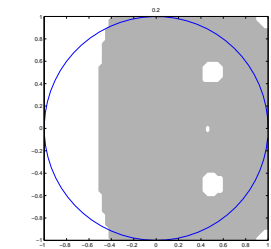
(d) Particles of  $St=0.05$



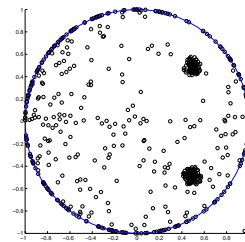
(e) Sensitivity field for  $St=0.1$



(f) Particles of  $St=0.1$



(g) Sensitivity field for  $St=0.2$



(h) Particles of  $St=0.2$

Figure 4.5: Relative velocity sensitivity field for particles over a range of stokes numbers (Left) and the corresponding distribution of a set of particles after time 't'(Right)

the microfluidic channel acts as perturbations of the relative velocity and increases the number of particles in the focused band.

## 4.4 A New Criteria For Inertial Particles To Settle Down Onto Streamlines

There are two well known criteria for identifying regions in which inertial particles settle in a flow field.

- Regions where eigen values of the Jacobian of the flow field are real and negative such as in areas outside of the gray-sensitive ( $Re(\lambda) - (2/3St) > 0$ ) region on the binary plots.
- Regions such as vortex cores, where the Jacobian of the flow field are purely imaginary.

We propose a third region in the four dimensional phase space Eq(2.27), where particles may potentially settle down. Regions with both positive and negative eigen values can also act as attractors for particles (i.e) for some initial conditions the particles may settle down in the regions that are neither vortex cores nor regions with purely negative eigen values. This happens if the dynamics of the particle ensures that the particle stay in regions where the rotation of eigen vectors of the term  $-(j + \mu I)$  in the simplified maxey riley equation eq(2.24) is large. A plot of the angle  $\theta$  by which the unstable eigen vector of the quantity  $-(j + \mu I)$  in Eq(2.24) rotates about the x axis at various points of the 2D plane of flow in a four vortex cell has been plotted in Figure(4.6). If the particle's initial conditions are such that the trajectory of the particle traverses through high  $\theta$  regions, then it ensures that

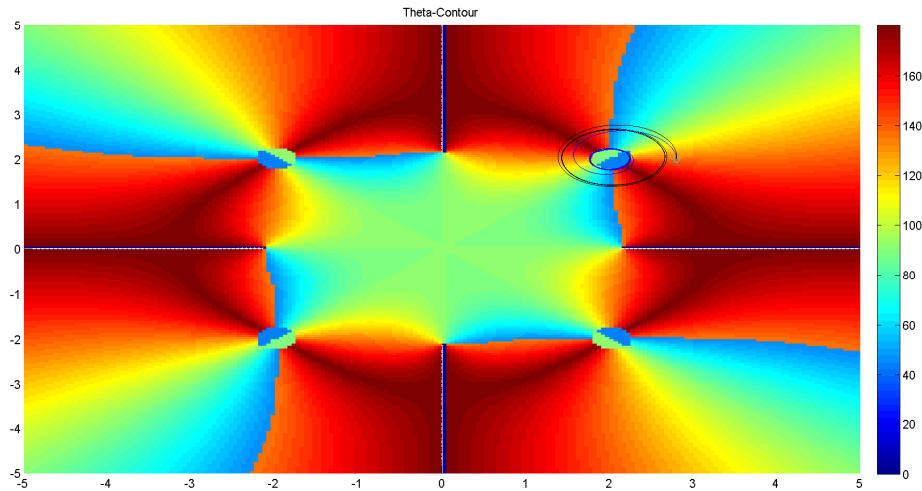
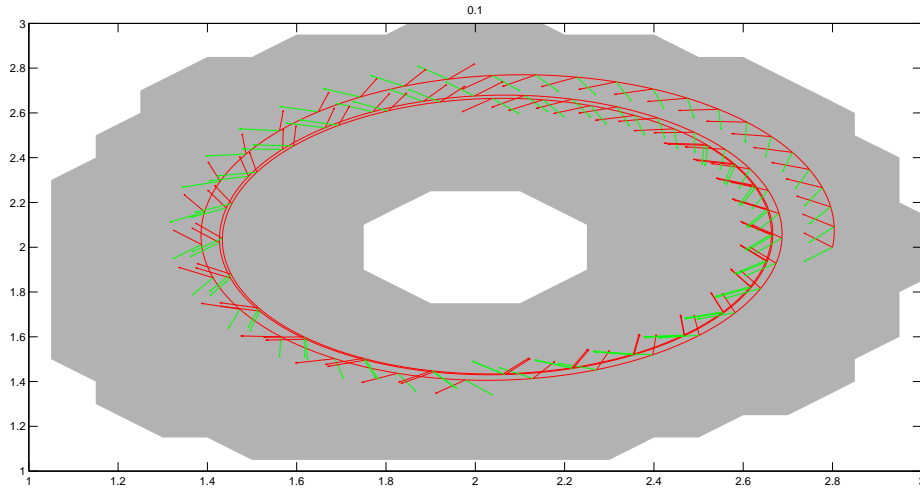


Figure 4.6: A contour of the angle  $\theta$  by which the unstable eigen vector of  $-(j + \mu I)$  rotates about the x-axis with special case and normal trajectories of a particle superimposed

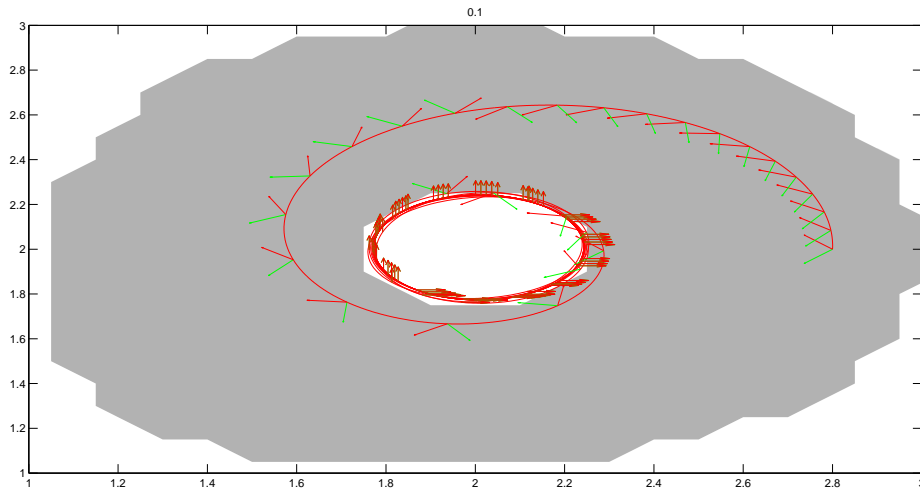
the particle's relative velocity decays in an oscillatory manner. The mechanism of relative velocity decay is explained next.

#### 4.4.1 Mechanism of relative velocity decay in regions of high eigen vector rotation

Two trajectories of a particle starting from the same point but with different relative velocities is shown in Figure(4.7). In Figure(4.7(b)), the particle behaves as expected and ends up inside the vortex core, but in Figure(4.7(a)), the particle settles down on a periodic orbit around the vortices inside the region with a positive value for  $Re(\lambda) - (2/3St)$ . This can be explained by looking at the eigen vectors of the right hand side of eq(2.24) which have been superimposed on the trajectories in Figure(4.7). The stable eigen vector is colored red and the unstable eigen vector is colored green.



(a) Special case trajectory of particles losing relative velocity inside  $Re(\lambda) - (2/3St) > 0$  region



(b) Normal trajectory of a particle inside  $Re(\lambda) - (2/3St) > 0$  region

Figure 4.7: Trajectories of a particle starting from different initial conditions in the 4 dimensional phase space

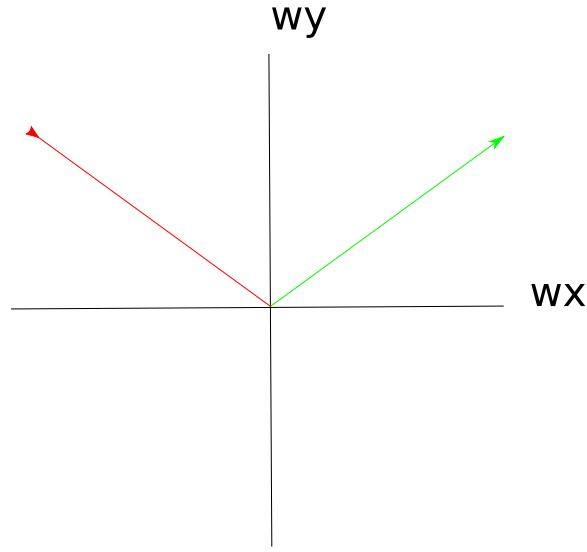
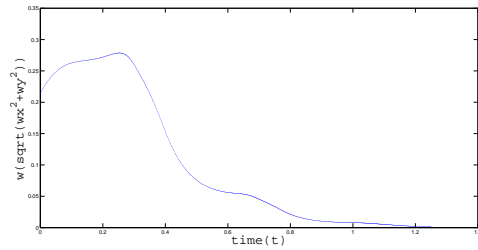


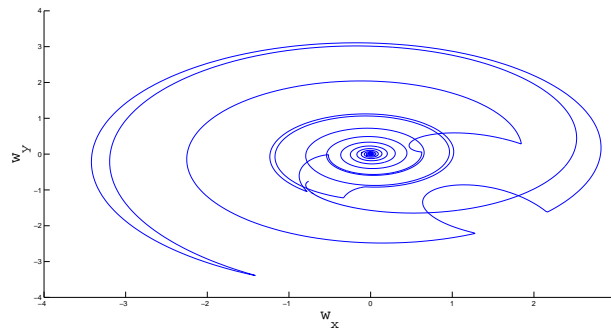
Figure 4.8: Eigen vectors of relative velocity

For the case of the special case trajectory which settles down in the positive  $Re(\lambda) - (2/3St)$  region, we see that the stable eigen vector corresponding to the negative eigen value and the unstable eigen vector corresponding to the positive eigen value rotate about the axes to a large extent unlike in the normal trajectory. Depending on the orientation of these eigen vectors, a particular component of the relative velocity ( $w_x$  or  $w_y$ ) may be more influenced by either the stable or unstable eigen vector Figure(4.8).

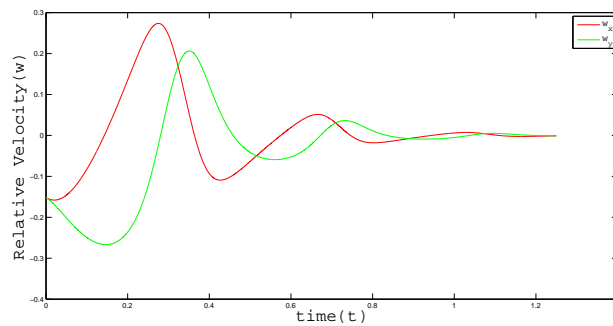
These large rotations of the eigen vectors ensure that each of the relative velocity components are influenced in a cyclic manner by both the stable and unstable eigen vectors, causing the values of  $w_x$  and  $w_y$  to rise and fall. However, by definition,  $|\lambda - (2/(3St))| < |-\lambda - (2/(3St))|$  and hence the influence of the stable eigen vector is greater on both components of relative velocity which implies that the cyclic rise and fall of  $w_x$  and  $w_y$  is accompanied by a decay of net relative velocity  $w$  Figure(4.9(a)) until all of the relative velocity decays Figure(4.9(b),c)) .



(a) The relative velocity decays with time for trajectories of the special case



(b) Trajectories of the  $w_x$ - $w_y$  phase space



(c) Components of relative velocity in the X and Y direction decaying with time

Figure 4.9: Relative Velocities of a particle starting from different initial conditions in the 4 dimensional phase space

# Chapter 5

## Conclusions and Future Work

Separation of inertial particles by size is very important for several processes in bio-engineering and chemical engineering and inertial particle dynamics is also of interest in oceanography and atmospheric flow studies. We have studied the dynamics of inertial particles numerically, in the presence of vorticity-a phenomenon present in many flows of interest. A method to selectively capture large particles in a mixture of particles of various sizes using an array of four vortex cells has been designed. The empirical observation of size based focusing of particles in curved micro-channels has been investigated. The effect of dean vortices on particle dynamics has been studied and the size based focusing behavior is numerically modeled.

A new mechanism by which inertial particles can lose their ability to cut across streamlines of flow and behave as fluid tracers instead has been introduced. The criteria to identify initial conditions in phase space which make particles lose their relative velocities by the new mechanism proposed has also been put forth.

As a suggestion for future work in this area, we believe that calculating the finite time lyapunov exponents(FTLE)of a large ensemble of particles in the flow configurations studied would enable us to identify subsets of the flow field where

particles have either a high or a low sensitivity to random perturbations of their relative velocity. The ridges of the sensitivity field form transport barriers(Lagrangian Coherent Structures). This information can be useful in designing particle mixers or separators.



# Bibliography

- [1] A. M Ardekani and R.H Rangel. Numerical investigation of particleparticle and particlewall collisions in a viscous fluid. *J. Fluid Mech*, 596:437–466, 2008.
- [2] H. Aref. Stirring by chaotic advection. *J.Fluid Mech*, 143:1–21, 1984.
- [3] A. Babiano, J.H.E Cartwright, O. Piro, and A. Provenzale. Dynamics of a small neutrally buoyant sphere in a fluid and targeting in hamiltonian systems. *Physical Review Letters*, 84(25), 2000.
- [4] A.B. Basset. *Treatise On Hydrodynamics*, volume 2. Deighton Bell, London, 1888.
- [5] Ali Asgar S. Bhagat, Sathyakumar S. Kuntaegowdanahalli, and I. Papautsky. Continuous particle separation in spiral microchannels using dean flows and differential migration. *Lab On a Chip*, 2008.
- [6] Ali Asgar S. Bhagat, Sathyakumar S. Kuntaegowdanahalli, and I. Papautsky. Inertial microfluidics for continuous particle filtration and extraction. *Microfluid Nanofluid*, 2009.
- [7] J. Boussinesq. *Theorie Analytique de la Chaleur*, volume 2. 1903.
- [8] D. Di Carlo, D. Irimia, R.G. Tompkins, and M. Toner. Continuous inertial focusing, ordering, and separation of particles in microchannels. *Proceedings Of The National Academy Of Sciences*, 2007.
- [9] Tchen Chan-Mou. *Mean Value and Correlated problems connected with the motion of small particles suspended in a turbulent flow*. PhD thesis, Technische Universiteit Delft, 1947.
- [10] K. Chong, S.D. Kelley, S. Smith, and J.D. Elridge. Inertial particle trapping in viscous streaming. *Physics of Fluids*, 2013.
- [11] W. R. Dean. Mathematical, physical and engineering sciences. *Proceedings of the Royal Society A*, (121):402–420, 1928.

- [12] Lindsey K. Fiddes, Neta Raz, Suthan Sriganapalan, Ethan Tumarkan, Craig A. Simmons, Aaron R. Wheeler, and Eugenia Kumacheva. A circular cross-section pdms microfluidics system for replication of cardiovascular flow conditions. *Bio-materials*, 2010.
- [13] H. Helmholtz. "über integrale der hydrodynamischen gleichungen, welche den wirbelbewegungen entsprechen". *J.Reine Angew. Math.*, 55(25-55), 1858.
- [14] J. Holtmark, I. Jonsen, T. Sikkeland, and S. Skavlem. Boundary layer flow near a cylindrical obstacle in an oscillating, incompressible fluid. *The Journal Of The Acoustical Society of America*, 1954.
- [15] Pijush K. Kundu and Ira M. Cohen. *Fluid Mechanics*. Academic Press, second edition, 2002.
- [16] L.M. Milne-Thomson. *Theoretical Hydrodynamics*. Macmillan and Co Ltd, 1968.
- [17] J.M. Martel and M. Toner. Particle focusing in curved microfluidic channels. *Nature-Scientific Reports*, 2013.
- [18] M. Maxey and J. Riley. Equation of motion for a small rigid sphere in nonuniform flow. *Physics Of Fluids*, 1983.
- [19] Paul K. Newton. *The N-Vortex Problem: Analytical Techniques*. Springer, 2001.
- [20] C.W. Oseen. *Hydrodynamik*. 1927.
- [21] P.G. Saffman. *Vortex Dynamics*. Cambridge University Press, 1992.
- [22] P. Tallapragada, N. Hasabnis, K. Katuri, S. Sudarsanam, K. Joshi, and M. Ramasubramanian. Scale invariant hydrodynamic focusing and sorting of inertial particles by size in spiral micro channels. *Journal of Micromechanics and Microengineering*(Accepted for publication).
- [23] C. Eugene Wayne. Vortices and two-dimensional fluid motion. *Notices of the AMS*, 58(1), 2011.